

Highly Specific and Broadly Potent Inhibitors of Mammalian Secreted Phospholipases A₂Rob C. Oslund,[†] Nathan Cermak,[†] and Michael H. Gelb^{*,†,‡}

Departments of Chemistry and Biochemistry, University of Washington, Seattle, Washington 98195

Received April 11, 2008

We report a series of inhibitors of secreted phospholipases A₂ (sPLA₂s) based on substituted indoles, 6,7-benzoindoles, and indolizines derived from LY315920, a well-known indole-based sPLA₂ inhibitor. Using the human group X sPLA₂ crystal structure, we prepared a highly potent and selective indole-based inhibitor of this enzyme. Also, we report human and mouse group IIA and IIE specific inhibitors and a substituted 6,7-benzoindole that inhibits nearly all human and mouse sPLA₂s in the low nanomolar range.

Introduction

Secreted phospholipases A₂ (sPLA₂s)¹ are a family of disulfide-rich, Ca²⁺-dependent enzymes that hydrolyze the *sn*-2 position of glycerophospholipids to release a fatty acid and a lysophospholipid.¹ The mouse genome encodes 10 sPLA₂s (groups IB, IIA, IIC, IID, IIE, IIF, III, V, X, XIIA), whereas the human genome encodes all of these except the group IIC enzyme, which occurs as a pseudogene.^{2,3} More than a decade ago there was interest in human group IIA sPLA₂ (hGIIA) as an anti-inflammatory drug target because it was found at high concentrations in synovial fluid from arthritis patients,⁴ although a clinical trial with an inhibitor against hGIIA failed to show efficacy in the treatment of rheumatoid arthritis.⁵ Interest in inhibitors of sPLA₂s has remained because of the possible involvement of these enzymes in inflammation. For example, studies with mGX- and mGV-deficient mice show that these sPLA₂s contribute to airway inflammation in a mouse model of allergic asthma.^{6,7} Studies with macrophages from mGV-deficient mice show a partial reduction in eicosanoid production in response to agonists.⁸

Substituted indoles and indolizines first reported by workers at Lilly and Shionogi are the most potent sPLA₂ inhibitors and the ones with drug potential in terms of pharmacokinetic profiles. Compounds in this group include the indolizine Indoxam and the substituted indoles Me-Indoxam and **1** (LY315920; Figure 1).^{9–12} The development of these compounds is an early example of structure-guided improvement of binding potency starting from a lead compound obtained through high-throughput screening¹³ and making use of the X-ray structure of hGIIA.¹⁴

With the availability of the full set of mouse and human recombinant sPLA₂s, it has been recently possible to explore the specificity of these compounds against all mammalian family members.^{15–17} For example, Me-Indoxam inhibits hGIIA, mGIIA, mGIIC, hGIIIE, mGIIE, hGV, and mGV sPLA₂s with low nanomolar potency, is less potent on hGIB, mGIB, hGX, and mGX, and inhibits hGIID, mGIID, hGXIIA, and mGXIIA only at micromolar concentrations.¹⁵ Compound **1** potently inhibits hGIIA, mGIIA, hGIIIE, mGIIE, hGX, and mGX enzymes and is less potent on the other mammalian

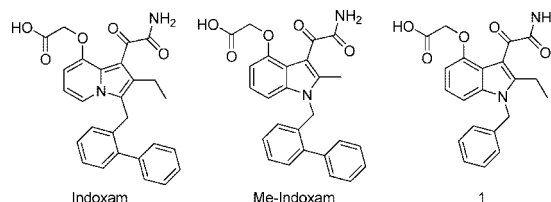


Figure 1. Substituted indole and indolizine sPLA₂ inhibitors.

sPLA₂s.¹⁷ In the current study we have taken a structure-guided approach using the X-ray structure of hGX^{16,18} to obtain inhibitors in the class shown in Figure 1 that are highly specific for hGX. Along the way we also obtained a highly specific inhibitor that binds only to hGIIA, mGIIA, hGIIIE, and mGIIE as well as a broadly potent inhibitor that shows strong inhibition against human and mouse GIB, GIIA, GIID, GIIE, GIIF, GV and GX sPLA₂s. These compounds may be useful in the study of the role of various mammalian sPLA₂s in cellular and whole animal responses.

Chemistry

Reported compounds were prepared using slightly modified routes.^{9–12,17,19} The substituted indole and 6,7-benzoindole inhibitors were prepared using analogous routes starting from 2-carbomethoxy-4-methoxy-indole **4a** and 2-carbomethoxy-4-methoxy-6,7-benzoindole **4b**, respectively. However, because **4b** could not be purchased commercially, it was prepared from commercially available 3-methoxy-2-naphthalenemethanol **2a** (Scheme 1). 3-Methoxy-2-naphthalenemethanol (**2a**) was oxidized with PCC to form the aldehyde **2b**. The aldehyde was treated with methyl azidoacetate and sodium methoxide to form the azidocinamate **3**. Ring closure of **3** was achieved via the Hemetsberger reaction to give 2-carbomethoxy-4-methoxy-6,7-benzoindole **4b**.

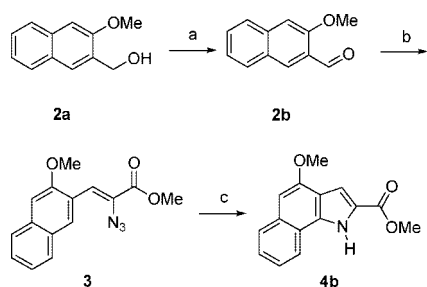
Indole-based inhibitors **11c**, **11d**, **12a**, and **12b** were prepared by N-1 benzylation of commercially available **4a** using sodium hydride as the base to yield **5a** (Scheme 2). The methyl ester was saponified to form the 2-carboxylic acid indole **6a**. The 2-acetyl indole **7a** was formed by treatment of **6a** with methyllithium. Reduction of the ketone was carried out with NaBH₄ to yield **8a**. Deoxygenation of **8a** was achieved using a mixture of NaBH₄ and trifluoroacetic acid to give **9a**. The 2-isobutyl indole intermediate **9b** was prepared in a similar fashion as **9a** except isobutyllithium was used in place of methyllithium to form **7b** with subsequent transformations to give **9b**. Compounds **10a–d** were prepared by first deprotecting

* To whom correspondence should be addressed. Tel.: 206-543-7142. Fax: 206-685-8665. E-mail: gelb@chem.washington.edu.

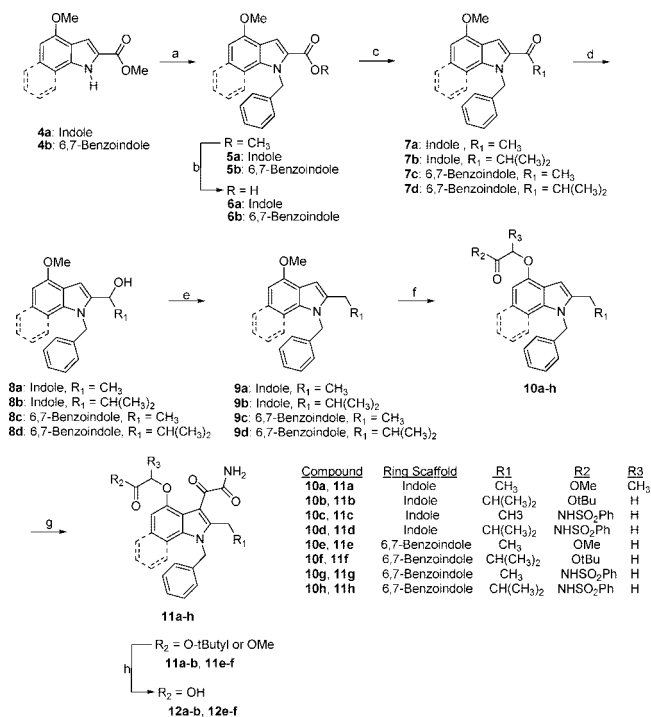
[†] Department of Chemistry.

[‡] Department of Biochemistry.

^a Abbreviations: hGIIA, human group IIA secreted phospholipase A₂ (likewise for other group names); mGIIA, mouse group IIA secreted phospholipase A₂ (likewise for other group names); sPLA₂, secreted phospholipase A₂.

Scheme 1^a

^a Reagents and conditions: (a) PCC, NaAcetate in CH₂Cl₂; (b) methyl azidoacetate, NaOMe in THF; (c) xylene or toluene, reflux.

Scheme 2^a

^a Reagents and conditions: (a) NaH, BnBr in DMF; (b) 30% KOH/MeOH/THF (2:1:1), reflux; (c) MeLi or isopropyllithium in THF; (d) NaBH₄ in EtOH/THF; (e) NaBH₄, TFA in CH₂Cl₂; (f) (1) BBr₃ in CH₂Cl₂, (2) NaH R₂COCHR₃Br in DMF; (g) (1) oxalyl chloride in CH₂Cl₂, (2) NH₃(g); (h) 1.5 M NaOH in MeOH/THF or 20% TFA in CH₂Cl₂.

the 4-methoxy substituent on **9a** and **9b** using BBr₃ followed by addition of the appropriate alkyl bromoacetate or 2-bromo-*N*-(arylsulfonyl)acetamide with sodium hydride as the base. Addition of the oxalamide group to the indole was carried out by treating **10a–d** with oxalyl chloride followed by addition of ammonia gas to give compounds **11a–d**. Deprotection of the indole esters **11a** and **11b** was carried out with NaOH to give **12a** or with trifluoroacetic acid to yield **12b**.

Preparation of the 6,7-benzoindoles **11g**, **11h**, **12e**, and **12f** was done using identical routes described for the substituted indole inhibitors (Scheme 2). Compounds **14a** and **14b**, *N*-methyl amides **15a** and **15b**, and all **11d** derivatives were prepared using analogous steps to those outlined in Scheme 2. All Indoxam derivatives (**15c** and **16a–c**) were prepared using similar techniques to those already described.¹²

Results and Discussion

Molecular Modeling. We recently reported that compound **1** was 30 times more potent than the 2-methyl indole against

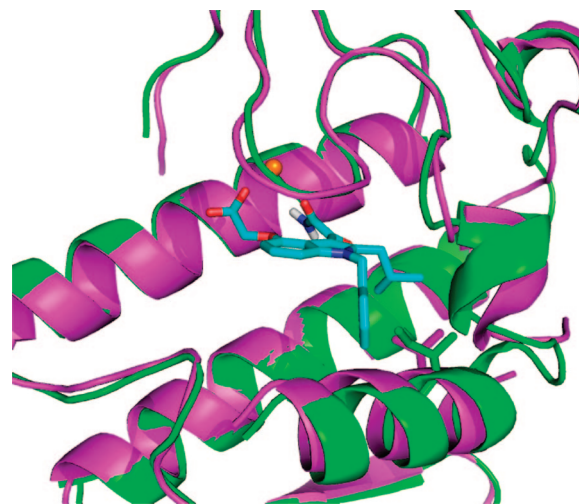
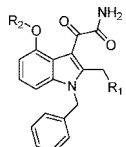


Figure 2. An overlay of hGIIA (green) and hGX (magenta) with **12b** docked into the active site. The isoleucine of hGIIA, but not the valine of hGX, provides extra hydrophobic bulk near the 2-isobutyl group on the indole ring and presumably excludes the 2-isobutyl indole from the active site.

hGX.¹⁷ We explored this gain in selectivity by docking indole compounds with larger 2-alkyl groups into the hGIIA and hGX sPLA₂ active sites of existing X-ray crystal structures^{13,16} using the FLO/QXP docking program.²⁰ An overlay of the hGIIA and hGX enzyme structures (rms C_α = 0.98 Å) revealed a region of extra space in the hGX active site not present in hGIIA. This difference in hydrophobic space results mostly from a change in one amino acid residue. hGIIA has an isoleucine whereas hGX has a valine in the active site region which is contacted by the 2-position substituent on the indole ring (Figure 2). Larger 2-alkyl substituents would clash with this portion of the hGIIA active site but not in the case of hGX. Our designs were supported by data from workers at Shionogi showing that 2-isobutyl indole and indole-like inhibitors selectively inhibited the hGX enzyme.²¹ However, this report only included IC₅₀ values for these compounds against hGIB, hGIIA, hGV, and hGX. As a group X specific inhibitor would be extremely useful, we wanted to test 2-isobutyl indole derivatives against all human and mouse sPLA₂ enzymes.

Also, in attempts to increase hydrophobicity of these compounds in order to make them more cell permeable, docking studies revealed that larger substituents such as arylsulfonamides or alkylsulfonamides could replace the carboxylic acid OH group on the indole scaffold. In our previous studies, addition of a methyl group to the 6-position on the indole scaffold did not affect inhibition potency against the various sPLA₂s tested.¹⁷ Larger groups including a benzene ring fused to the 6,7-position of the indole scaffold were also docked into the active site without affecting key binding interactions.

In Vitro Inhibitor. Using a fluorometric sPLA₂ assay,¹⁶ the substituted indoles, 6,7-benzoindoles, and indolizines were tested against the full panel of human and mouse sPLA₂ enzymes, with the exception of mGIIC (because humans contain a group IIC pseudogene) and mGXIII, which has 94% sequence identity to hGXIII.¹⁵ All reported compounds in this study except **13a–i**, **14b**, and **15a–c** were tested against hGIII and hGXIII sPLA₂ enzymes, and gave <50% inhibition for both enzymes at 1.6 μM concentrations. The active sites of GIII and GXIII sPLA₂ are predicted to be significantly different than those of the other mammalian sPLA₂s, and this probably explains why the indole/indolizine set of inhibitors lack potency on GIII and GXIII enzymes. IC₅₀ values generated against hGIID were

Table 1. IC₅₀ Values of Substituted Indole Inhibitors against Human and Mouse sPLA₂s^a


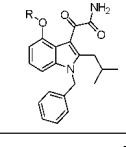
comp	R1	R2	IC ₅₀ (nM)													
			hGIB	mGIB	hGIIA	mGIIA	hGIID ^c	mGIID	hGIIE	mGIIE	hGIIF	mGIIF	hGV	mGV	hGX	mGX
1 ^b			750±150	140±75	125±20	70±20	60±10	430±90	50±20	75±20	130±30	>1600	500±50	750±100	75±10	75±10
11c			>1600	950±80	250±20	60±10	170±30	890±45	7±1	12±2	1100±60	>1600	100±20	60±7	15±3	30±7
11d			>1600	>1600	>1600	>1600	700±230	>1600	>1600	>1600	>1600	>1600	>1600	>1600	21±7	>1600
12a			80±20	100±30	170±40	60±10	120±40	>1600	9±4	140±50	90±30	470±190	44±9	57±20	22±2	20±5
12b			>1600	580±10	>1600	>1600	500±90	>1600	1300±18	>1600	550±100	>1600	>1600	>1600	50±16	>1600

^a IC₅₀ values are reported as the mean of duplicate or triplicate analysis with standard deviations. Each compound was screened at 1660 nM and reported as >1600 nM if the inhibition was <50%. ^b IC₅₀ values for GIB, GIIA, GIIE, GV, and GX from ref 17. Retest of this compound against hGV and mGV gave 110 ± 30 and 160 ± 20 nM, respectively. ^c IC₅₀ values obtained using *E. coli* membrane assay. Each compound was screened at 1330 nM and reported as >1300 nM if the inhibition was <50%.

obtained using the [³H]oleic acid-labeled *E. coli* membrane assay, which was preferred for this enzyme because of the higher sensitivity achieved over the fluorometric assay. Data in Table 1 show that **11d** and **12b** are highly selective for hGX over all other human and mouse sPLA₂s. Thus, the large isobutyl group is well tolerated only by hGX, which is consistent with modeling studies. Interestingly, these compounds lack potency against mGX despite the fact that hGX and mGX share 72% sequence identity. Structural alignment reveals that mGX does not contain a valine in the active site region that contacts the indole 2-position like hGX, but rather a leucine. This extra hydrophobic bulk sterically excludes the 2-isobutyl indoles from the mGX active site in similar fashion as with GIIA. Other sPLA₂s such as GIB, GIIE, and GV also have an isoleucine in this region like the GIIA enzyme. However, GIID and GIIF have a valine in this region like human GX, which supports the fact that the 2-isobutyl compounds **11h** and **12f** display somewhat increased potency against GIID and GIIF enzymes.

A small subset of **11d** derivatives were synthesized and tested against hGX sPLA₂ (Table 2). As initial docking studies predicted that the phenylsulfonamide group would extend out of the active site, it was surprising to see a 38-fold difference in inhibition for compounds **13b–d** when the phenyl ring was substituted with a chlorine at the *para*-, *meta*-, and *ortho*-positions (Table 2). Compounds **13d**, and **13f**, with substitutions at the *ortho*-position with a chloro- or methyl- group, resulted in higher inhibition potency over **11d** (Table 2). It is possible that the extra methyl or chlorine groups pack into a small pocket of the active site, which would increase the binding affinity. However, replacing the phenylsulfonamide on **11d** with a methylsulfonamide (**13h**) also increases potency against hGX (Table 2). Without a crystal structure, it is difficult to conclude how this phenylsulfonamide is contacting the enzyme active site.

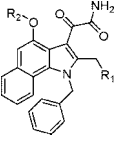
The 6,7-benzoindeole inhibitors display general potency against all tested human and mouse sPLA₂ enzymes (Table 3). Because the extra hydrophobic bulk is predicted not to make

Table 2. IC₅₀ Values of **11d** Derivatives against hGX sPLA₂^a


Comp	R	hGX
		IC ₅₀ (nM)
13a		80±10
13b		540±60
13c		140±30
13d		14±3
13e		320±30
13f		11±1
13g		70±20
13h		7±2
13i		30±10

^a IC₅₀ values are reported as the mean of duplicate or triplicate analysis with standard deviations.

direct contact with the enzyme, the increased potency is likely due to increased partitioning of the inhibitor into the phospho-

Table 3. IC₅₀ Values of Substituted Benzo-Fused Indole Inhibitors against Human and Mouse sPLA₂s^a


comp	R1	R2	IC ₅₀ (nM)													
			hGIB	mGIB	hGIIA	mGIIA	hGIID ^b	mGIID	hGIIIE	mGIIIE	hGIIF	mGIIF	hGV	mGV	hGX	mGX
11g			1300±290	1000±40	100±20	90±20	35±10	1000±590	16±1	48±9	550±120	>1600	140±6	70±10	90±20	35±5
11h			>1600	920±180	>1600	>1600	270±150	530±30	840±290	>1600	290±50	450±120	>1600	>1600	30±4	>1600
12e			84±3	160±40	40±2	30±1	7±3	320±5	7±2	18±2	50±3	170±33	35±7	20±1	20±3	6±1
12f			1400±40	290±20	>1600	>1600	80±20	640±190	260±10	1500±170	90±10	130±20	>1600	>1600	10±2	>1600
14a			810±80	1600±30	14±2	34±1	240±4	>1600	20±6	150±4	>1600	>1600	>1600	>1600	1500±270	>1600

^a IC₅₀ values are reported as the mean of duplicate or triplicate analysis with standard deviations. Each compound was screened at 1660 nM and reported as >1600 nM if the inhibition was <50%. ^b IC₅₀ values obtained using *E. coli* membrane assay. Each compound was screened at 1330 nM and reported as >1300 nM if the inhibition was <50%.

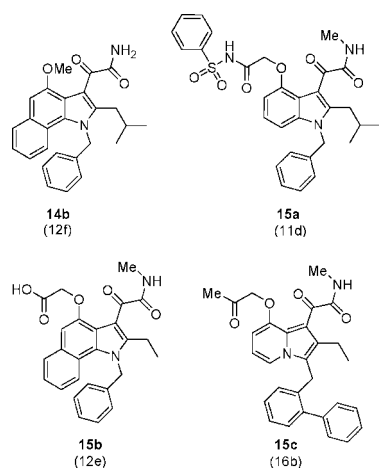


Figure 3. Control compounds designed by removing the functionality from the 4-position (**14b**) or by methylating the oxalamide (**15a–c**). Control compounds are >30-fold less potent than their parent compound (listed below the compound in parenthesis) when tested against hGX (**14b** and **15a**), human and mouse GIIA, GV, and GX (**15b**), or human GIIA (**15c**).

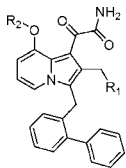
lipid substrate vesicles, which increases the ratio of X_i/K_i^* (X_i is the mole fraction of inhibitor in the interface and K_i^* is the interfacial dissociation constant).^{22,23} Of particular note is compound **12e** that inhibited human and mouse groups IB, IIA, IID, IIE, IIF, V, and X sPLA₂s with an IC₅₀ of less than 350 nM (Table 3). We also sought structurally similar compounds that would be devoid of sPLA₂ binding activity because such compounds are useful as controls in cellular studies. The X-ray structure of an Indoxam analogue bound to hGIIA and Me-Indoxam bound to hGX show that the carboxyl group of the substituent at the 4-position of the indole directly coordinates to the active site Ca²⁺.^{16,24} We thus synthesized **14a** and **14b** with only a methoxy group at the 4-position to remove the interaction made between the inhibitor and Ca²⁺. Surprisingly, while **14b** (Figure 3) gave an IC₅₀ of 1000 nM against hGX (data not included in table), **14a** had an IC₅₀ of 14 and 34 nM against human and mouse GIIA, respectively (Table 3).

Compound **14a** was also potent against hGIIIE and mGIIIE, consistent with trends observed for other potent group IIA indole-based inhibitors. Poor inhibiting control compounds were successfully designed by introduction of an N-methyl group on the oxalamide of the indole scaffold to give compounds **15a–15c** (Figure 3). Analysis of the co-crystal structure containing Me-Indoxam in the hGX active site reveals that the introduced N-methyl group disrupts a key hydrogen bond with either a histidine or aspartate residue, while also introducing extra hydrophobic bulk into the active site.¹⁶ All N-methyl oxalamide control compounds had IC₅₀ values that were >30-fold higher than their parent compound (Figure 3).

The 2-isobutyl Indoxam derivative **16a** was synthesized and found to poorly inhibit sPLA₂ enzymatic activity (Table 4). Since Indoxam does not inhibit hGX in the low nanomolar range (Table 4), it is not surprising that **16a** fails to inhibit hGX. This result suggests that poor inhibition of hGX activity by Indoxam or its derivatives has more to do with the indolizine heterocycle and not the substituents present on the ring. Interestingly, the 8-oxopropanone derivative **16b** and the 8-methoxy derivative **16c** were selectively potent against hGIIA and hGIIIE which was similar to the gain in selectivity displayed by **14a**. We also prepared **15c** (Figure 3), which did not significantly inhibit hGIIA at concentrations below 1600 nM.

Conclusion

A series of indole- and indolizine-based compounds were synthesized and tested against the full set of human and mouse sPLA₂ enzymes. Compound **11d** was found to be selectively potent against hGX over all other human and mouse sPLA₂ enzymes. Derivatives of **11d**, such as **13h**, were also found to bind with higher affinity to the hGX enzyme active site and may help in further studies of hGX sPLA₂ function. An inhibitor selective for mouse and human GIIA and GIIIE sPLA₂ (**14a**) as well as selective human GIIA and GIIIE inhibitors (**16b** and **16c**) were also identified from this group of compounds. Compound **12e** is potent against human and mouse groups IB, IIA, IID, IIE, IIF, V, and X and is the most generally potent sPLA₂ inhibitor reported to date. It is also the first reported potent

Table 4. IC₅₀ Values of Substituted Indolizine Inhibitors against Human and Mouse sPLA₂s^a


comp	R1	R2	IC ₅₀ (nM)													
			hGIB	mGIB	hGIIA	mGIIA	hGIID ^b	mGIID	hGIII	mGIII	hGIIF	mGIIF	hGV	mGV	hGX	mGX
Indoxam			700±30	1000±60	60±10	150±40	>1300	>1600	10±2	35±15	>1600	>1600	100±5	170±10	>1600	900±300
16a			>1600	>1600	>1600	>1600	>1300	>1600	>1600	>1600	970±50	1100±200	>1600	>1600	>1600	>1600
16b			>1600	1200±110	30±10	>1600	>1300	>1600	90±15	410±20	>1600	>1600	>1600	>1600	>1600	>1600
16c			>1600	320±20	35±2	>1600	>1300	>1600	50±10	230±110	>1600	>1600	>1600	>1600	>1600	>1600

^a IC₅₀ values are reported as the mean of duplicate or triplicate analysis with standard deviations. Each compound was screened at 1660 nM and reported as >1600 nM if the inhibition was <50%. ^b IC₅₀ values obtained using *E. coli* membrane assay. Each compound was screened at 1330 nM and reported as >1300 nM if the inhibition was <50%.

inhibitor of groups IID and IIF sPLA₂s. The inhibitors we describe may be useful in probing the roles of sPLA₂s in inflammatory diseases such as asthma and arthritis.

Experimental Section

Enzyme Inhibition Assays. For compounds with IC₅₀s <1600 nM in the fluorometric assay or <1300 nM in the *E. coli* membrane assay, inhibitor concentrations were varied with five different concentrations used to determine IC₅₀ values. All IC₅₀ values were obtained by nonlinear regression curve-fitting of percent inhibition versus log [inhibitor] using the Kaleidagraph software.

Fluorometric Assay. Microtiter plate assay of sPLA₂s using pyrene-labeled phosphatidylglycerol as the substrate was performed as described previously¹⁶ with the exception that seven wells were used per assay instead of eight.

***E. coli* Membrane Assay.** IC₅₀ values calculated for hGIID were done using a modified procedure from that reported previously.²⁵ See Supporting Information for details.

Synthesis. All reagents were purchased from Sigma-Aldrich and used directly unless otherwise stated. Reactions were performed under an atmosphere of dry nitrogen in oven-dried glassware. Reactions were monitored for completeness by thin layer chromatography (TLC) using Merck 60F₂₅₄ silica plates, and column chromatography was done with 60 Å silica gel purchased from Silicycle. ¹H NMR spectra were recorded on dilute solutions in CDCl₃, CD₃OD, or DMSO-*d*₆. NMR spectra were obtained on a Bruker AC-300 (300 MHz) and electrospray ionization mass spectra were acquired on a Bruker Esquire LC00066 for all compounds. Preparative reverse phase HPLC was performed on an automated Varian Prep Star system using a YMC S5 ODS column (20 × 100 mm, Waters Inc.).

Representative Procedure for Synthesis of Substituted 6,7-Benzindole Inhibitors (Compound 12e): Preparation of 1-Benzyl-2-carbomethoxy-4-methoxy-6,7-benzindole (5b). Compound **4b** (synthesis described in Supporting Information; 800 mg, 3.14 mmol) was dissolved in 10 mL dry DMF and stirred at 0 °C and sodium hydride (140 mg, 5.5 mmol) was added. After stirring for five minutes at 0 °C, benzylbromide (820 μL, 6.90 mmol) was added and the reaction was stirred for 30 min at room temperature. The reaction mixture was poured onto 20 mL of H₂O and 20 mL of EtOAc in a separatory funnel. The layers were separated and the organic layer was washed with 3 × 10 mL H₂O and the combined aqueous layer was back-extracted with 1 × 20 mL EtOAc. The combined organic layer was dried over MgSO₄ and filtered, and

the solvent was removed by rotary evaporation. The crude white solid was purified by column chromatography on silica gel (20% EtOAc/80% hexanes) to give a white solid (820 mg, 75% yield). ¹H NMR (300 MHz, CDCl₃) δ 3.85 (s, 3H), 4.06 (s, 3H), 6.34 (bs, 2H), 6.77 (s, 1H), 7.09 (d, *J* = 7.2 Hz, 2H), 7.16–7.31 (m, 4H), 7.37 (t, *J* = 7.2 Hz, 1H), 7.68 (s, 1H), 7.78 (d, *J* = 8.1 Hz, 1H), 8.06 (d, *J* = 8.4 Hz, 1H).

Preparation of 1-Benzyl-2-carboxylic acid-4-methoxy-6,7-benzindole (6b). Compound **5b** (485 mg, 1.41 mmol) was suspended in 15 mL of 30% KOH/MeOH/THF (2:1:1) and refluxed for 2.0 h (all the solid dissolved during reflux). After refluxing, the reaction was cooled on ice and the pH was made acidic using 2 N HCl, causing the product to precipitate. The white solid was collected by vacuum filtration and washed with 1 × 10 mL of cold water and 2 × 10 mL of cold hexanes to give a white solid (400 mg, 86% yield). ¹H NMR (300 MHz, DMSO-*d*₆) δ 4.02 (s, 3H), 6.41 (bs, 2H), 6.98 (m, 3H), 7.20–7.26 (m, 2H), 7.32 (t, *J* = 7.5 Hz, 2H), 7.39 (t, *J* = 8.1 Hz, 1H), 7.49 (s, 1H), 7.86 (d, *J* = 7.5 Hz, 1H), 8.12 (d, *J* = 8.4 Hz, 1H).

Preparation of 1-Benzyl-2-acetyl-4-methoxy-6,7-benzindole (7c). Compound **6b** (920 mg, 1.12 mmol) was dissolved in 40 mL of dry THF to which 6.6 mL of 1.25 M MeLi in diethyl ether was added dropwise and stirred at room temperature for 2.5 h. Saturated NH₄Cl (8 mL) was added followed by the addition of 2 N HCl until the mixture had an acidic pH. The reaction mixture was then poured onto 30 mL of EtOAc and 30 mL of H₂O in a separatory funnel. The layers were separated and the water phase was washed with 2 × 20 mL of EtOAc. The organic layers were combined, dried over MgSO₄ and filtered, and the solvent was removed by rotary evaporation. The crude white solid was triturated in 15 mL of 1:1 EtOAc/hexanes and separated from the solvent by vacuum filtration. The white solid collected via vacuum filtration was washed with 2 × 10 mL of 1:1 EtOAc/hexanes giving **6b**. Additional product could be purified from the combined filtrate and washings by removing the solvent and repeating the trituration step described above followed by chromatography on silica gel (20% EtOAc/80% hexanes) of the filtrate and washings combined together from the second trituration step. The purified product was combined to afford a white solid (366 mg, 40% yield). ¹H NMR (300 MHz, CDCl₃) δ 2.63 (s, 3H), 4.08 (s, 3H), 6.35 (bs, 2H), 6.77 (s, 1H), 7.07 (d, *J* = 6.9 Hz, 2H), 7.20–7.31 (m, 4H), 7.39 (t, *J* = 8.1 Hz, 1H), 7.67 (s, 1H), 7.78 (d, *J* = 8.1 Hz, 1H), 8.09 (d, *J* = 8.7 Hz, 1H).

Preparation of 1-(1-Benzyl-4-methoxy-1H-6,7-benzoindol-2-yl)-ethanol (8c). Compound **7c** (366 mg, 1.11 mmol) was dissolved in 30 mL of 75% EtOH/25% THF, and NaBH₄ (100 mg, 3.33 mmol) was added to the mixture and stirred at room temperature for 16 h. The reaction mixture was then poured onto 30 mL EtOAc and 30 mL H₂O in a separatory funnel. The layers were separated and the water phase was washed with 2 × 20 mL of EtOAc. The organic layers were combined and washed with 2 × 20 mL of H₂O and 1 × 20 mL of satd NaCl. The organic layer was dried over MgSO₄ and filtered, and the solvent was removed by rotary evaporation to give **8c** as a white solid that was used without further purification (355 mg, 96% yield). ¹H NMR (300 MHz, CDCl₃) δ 1.72 (d, *J* = 6.3 Hz, 3H), 4.08 (s, 3H), 4.99 (m, 1H), 5.96 (d, *J* = 20.7 Hz, 1H), 6.09 (d, *J* = 20.7 Hz, 1H), 6.81 (s, 1H), 6.85 (s, 1H), 7.05 (d, *J* = 6.9 Hz, 2H), 7.15 (t, *J* = 6.9 Hz, 1H), 7.20–7.31 (m, 4H), 7.79 (d, *J* = 8.1 Hz, 1H), 7.93 (d, *J* = 8.7 Hz, 1H).

Preparation of 1-Benzyl-2-ethyl-4-methoxy-1H-6,7-benzoindol-9c (9c). Compound **8c** (420 mg, 1.26 mmol) was dissolved in 20 mL of dry CH₂Cl₂ and added dropwise to a mixture of 14 mL of 99% trifluoroacetic acid (TFA) and NaBH₄ (243 mg, 6.3 mmol) at 20 °C (prepare TFA/NaBH₄ mixture in an ice bath by careful dropwise addition of TFA to NaBH₄ and let stir until NaBH₄ fully dissolves before raising temperature). The reaction mixture was stirred at room temperature for 30 min and then poured onto 30 mL of satd NaHCO₃ and 30 mL of CH₂Cl₂ in a separatory funnel. Once bubbling ceased, the layers were separated and the water phase was washed with 2 × 20 mL of CH₂Cl₂. The organic layers were combined, dried over MgSO₄ and filtered, and the solvent was removed by rotary evaporation. The crude material was purified by column chromatography on silica gel (20% EtOAc/80% hexanes) to afford a white solid (335 mg, 84% yield). ¹H NMR (300 MHz, CDCl₃) δ 1.36 (t, *J* = 7.5 Hz, 3H), 2.75 (q, *J* = 7.5 Hz, 2H), 4.07 (s, 3H), 5.77 (s, 2H), 6.56 (s, 1H), 6.80 (s, 1H), 7.05 (d, *J* = 6.9 Hz, 2H), 7.13 (t, *J* = 6.9 Hz, 1H), 7.20–7.31 (m, 4H), 7.79 (d, *J* = 8.1 Hz, 1H), 7.93 (d, *J* = 8.7 Hz, 1H).

Preparation of Methyl 2-(1-Benzyl-2-ethyl-1H-6,7-benzoindol-4-yloxy)acetate (10e). Compound **9c** (80 mg, 0.25 mmol) was dissolved in 8 mL of dry CH₂Cl₂ and stirred at 0 °C. BBr₃ (1.0 M in CH₂Cl₂; 635 μL, 0.635 mmol) was added in portions over 5 min to the reaction mixture at 0 °C, and the reaction mixture was stirred for 3 h at room temperature or until product formation was complete as indicated by TLC. H₂O (8 mL) was added to the reaction mixture to quench excess BBr₃, and the reaction mixture was poured onto 20 mL of CH₂Cl₂ and 20 mL of H₂O in a separatory funnel. The layers were separated and the water phase was washed with 2 × 20 mL of CH₂Cl₂. The organic layers were combined, dried over MgSO₄ and filtered, and the solvent was removed by rotary evaporation to give the 4-hydroxy-6,7-benzoindol intermediate, which is unstable and decomposes giving a purple color upon exposure to air. After drying in vacuo for 30 min, this compound was then immediately dissolved in 4 mL of DMF and stirred in an ice bath. Sodium hydride (10.3 mg, 0.41 mmol) was added to the reaction mixture and stirred 5 min at 0 °C, with subsequent addition of methyl bromoacetate (40 μL, 0.456 mmol). The reaction was stirred at room temperature for 30 min. Additional portions of sodium hydride were added at 0 °C until the reaction was shown to be complete by TLC. The reaction mixture was then poured onto 20 mL of H₂O and 20 mL of EtOAc in a separatory funnel. The layers were separated and the organic layer was washed with 4 × 10 mL of H₂O, and the combined aqueous layer was back-extracted with 1 × 20 mL of EtOAc. The combined organic layers were dried over MgSO₄ and filtered, and the solvent was removed by rotary evaporation. The crude material was purified by column chromatography on silica gel (20% EtOAc/80% hexanes) to afford a white solid (23 mg, 24% yield over two steps). ¹H NMR (300 MHz, CDCl₃) δ 1.37 (t, *J* = 7.5 Hz, 3H), 2.75 (q, *J* = 7.5 Hz, 2H), 3.85 (s, 3H), 4.90 (s, 2H), 5.76 (s, 2H), 6.69 (s, 1H), 6.76 (s, 1H), 7.05 (d, *J* = 6.9 Hz, 2H), 7.15 (t, *J* = 6.9 Hz, 1H), 7.20–7.31 (m, 4H), 7.75 (d, *J* = 8.1 Hz, 1H), 7.95 (d, *J* = 8.4 Hz, 1H).

Preparation of Methyl-2-(3-(2-amino-2-oxoacetyl)-1-benzyl-2-ethyl-1H-6,7-benzoindol-4-yloxy)acetate (11e). Compound **10e** (22.4 mg, 0.06 mmol) was dissolved in 7 mL of dry CH₂Cl₂ and added dropwise to 14 mL of dry CH₂Cl₂ containing oxalyl chloride (26 μL, 0.30 mmol) at room temperature. The reaction mixture was stirred overnight at room temperature. Ammonia gas was then bubbled into the reaction mixture for five minutes. The reaction mixture was then poured into a separatory funnel containing 20 mL of 2 N HCl. The layers were separated and the aqueous layer was extracted with 2 × 10 mL of CH₂Cl₂. The organic layers were combined, dried over MgSO₄ and filtered, and the solvent was removed by rotary evaporation. The crude mixture was purified by column chromatography over silica gel (70% EtOAc/30% hexanes) to give a white yellow solid (10.9 mg, 41% yield). ¹H NMR (300 MHz, CDCl₃) δ 1.23 (t, *J* = 7.5 Hz, 3H), 2.94 (q, *J* = 7.5 Hz, 2H), 3.81 (s, 3H), 4.88 (s, 2H), 5.42 (bs, 1H), 5.81 (s, 2H), 6.72 (bs, 1H), 6.81 (s, 1H), 7.10 (d, *J* = 6.9 Hz, 2H), 7.17 (t, *J* = 6.9 Hz, 1H), 7.20–7.31 (m, 4H), 7.74 (d, *J* = 7.8 Hz, 1H), 7.92 (d, *J* = 8.4 Hz, 1H). MS (ESI, pos. ion) *m/z*: 467 (M + Na⁺).

Preparation of 2-(3-(2-Amino-2-oxoacetyl)-1-benzyl-2-ethyl-1H-6,7-benzoindol-4-yloxy)acetic Acid (12e). Compound **11e** (10.9 mg, 0.024 mmol) was dissolved in 5 mL of MeOH/THF (5:1) with 0.5 mL of 1.5 M NaOH added to the reaction mixture and stirred for 2.5 h at room temperature. The reaction mixture was then poured onto 20 mL of 2 N HCl and 20 mL of CH₂Cl₂ in a separatory funnel. The layers were separated and the aqueous layer was extracted with 2 × 10 mL of CH₂Cl₂. The combined organic layer was dried over MgSO₄ and filtered, and the solvent was removed by rotary evaporation to yield **12e** quantitatively. A portion of **12e** was purified by HPLC using the following program (eluting solvents each contained 0.08% TFA): 0–5 min 30% MeOH/70% H₂O, 5–30 min 30% MeOH/70% H₂O–70% MeOH/30% H₂O, 30–32 min 70% MeOH/30% H₂O–100% MeOH, 32–35 min 100% MeOH. The product eluted at 24.5 min and the solvent was removed by Speed-Vac to afford a white/yellow solid (4.9 mg). ¹H NMR (300 MHz, MeOD) δ 1.26 (t, *J* = 7.2 Hz, 3H), 3.04 (q, *J* = 7.5 Hz, 2H), 4.93 (s, 2H), 5.99 (s, 2H), 6.96 (s, 1H), 7.15–7.23 (m, 3H), 7.27–7.39 (m, 4H), 7.83 (d, *J* = 6.9 Hz, 1H), 8.07 (d, *J* = 8.4 Hz, 1H). MS (ESI, pos. ion) *m/z*: 431 (M⁺).

Acknowledgment. The authors thank Justin Siegel and Drs. Brian Smart and Zhanlin Ni for helpful discussions about the inhibitors used in this work and Dr. Christophe Verlinde for modeling discussions. This work was supported by an NIH Molecular Biophysics Training Grant (R.C.O.), the Mary Gates Foundation (N.C.), and a Merit Award from the National Institutes of Health (M.H.G.; R37HL036235).

Supporting Information Available: Details of synthetic methods, including NMR and MS data, for all other described compounds, HPLC traces showing purity of key target compounds, molecular modeling details, and *E. coli* membrane enzyme assay procedures. This material is available free of charge via the Internet at <http://pubs.acs.org>.

References

- (1) Lambeau, G.; Gelb, M. H. Biochemistry and physiology of mammalian secreted phospholipases A₂. *Annu. Rev. Biochem.* **2008**, in press.
- (2) Valentin, E.; Lambeau, G. Increasing molecular diversity of secreted phospholipases A₂ and their receptors and binding proteins. *Biochim. Biophys. Acta* **2000**, *1488*, 59–70.
- (3) Six, D. A.; Dennis, E. A. The expanding superfamily of phospholipase A₂ enzymes: classification and characterization. *Biochim. Biophys. Acta* **2000**, *1488*, 1–19.
- (4) Pruzanski, W. Phospholipase A₂: quo vadis. *J. Rheumatol.* **2005**, *32*, 400–402.
- (5) Bradley, J. D.; Dmintrienko, A. A.; Kivitz, A. J.; Gluck, O. S.; Weaver, A. L.; Wiesenhutter, C.; Myers, S. L.; Sides, G. D. Randomized, double-blinded, placebo-controlled clinical trial of LY333013, a selective inhibitor of group II secretory phospholipases A₂, in the treatment of rheumatoid arthritis. *J. Rheumatol.* **2005**, *32*, 417–423.
- (6) Henderson, W. R., Jr.; Chi, E. Y.; Bollinger, J. G.; Tien, Y. T.; Ye, X.; Castelli, L.; Rubtsov, Y. P.; Singer, A. G.; Chiang, G. K.;

- Nevalainen, T.; Rudensky, A. Y.; Gelb, M. H. Importance of group X-secreted phospholipase A₂ in allergen-induced airway inflammation and remodeling in a mouse asthma model. *J. Exp. Med.* **2007**, *204*, 865–77.
- (7) Munoz, N. M.; Meliton, A. Y.; Arm, J. P.; Bonventre, J. V.; Cho, W.; Leff, A. R. Deletion of secretory group V phospholipase A₂ attenuates cell migration and airway hyperresponsiveness in immunosensitized mice. *J. Immunol.* **2007**, *179*, 4800–4807.
- (8) Satake, Y.; Diaz, B. L.; Balestrieri, B.; Lam, B. K.; Kanaoka, Y.; Grusby, M. J.; Arm, J. P. Role of group V phospholipase A₂ in zymosan-induced eicosanoid generation and vascular permeability revealed by targeted gene disruption. *J. Biol. Chem.* **2004**, *279*, 16488–16494.
- (9) Dillard, R. D.; Bach, N. J.; Draheim, S. E.; Berry, D. R.; Carlson, D. G.; Chirgadze, N. Y.; Clawson, D. K.; Hartley, L. W.; Johnson, L. M.; Jones, N. D.; McKinney, E. R.; Mihelich, E. D.; Olkowski, J. L.; Schevitz, R. W.; Smith, A. C.; Snyder, D. W.; Sommers, C. D.; Wery, J. P. Indole inhibitors of human nonpancreatic secretory phospholipase A₂. 1. Indole-3-acetamides. *J. Med. Chem.* **1996**, *39*, 5119–36.
- (10) Dillard, R. D.; Bach, N. J.; Draheim, S. E.; Berry, D. R.; Carlson, D. G.; Chirgadze, N. Y.; Clawson, D. K.; Hartley, L. W.; Johnson, L. M.; Jones, N. D.; McKinney, E. R.; Mihelich, E. D.; Olkowski, J. L.; Schevitz, R. W.; Smith, A. C.; Snyder, D. W.; Sommers, C. D.; Wery, J. P. Indole inhibitors of human nonpancreatic secretory phospholipase A₂. 2. Indole-3-acetamides with additional functionality. *J. Med. Chem.* **1996**, *39*, 5137–5158.
- (11) Draheim, S. E.; Bach, N. J.; Dillard, R. D.; Berry, D. R.; Carlson, D. G.; Chirgadze, N. Y.; Clawson, D. K.; Hartley, L. W.; Johnson, L. M.; Jones, N. D.; McKinney, E. R.; Mihelich, E. D.; Olkowski, J. L.; Schevitz, R. W.; Smith, A. C.; Snyder, D. W.; Sommers, C. D.; Wery, J. P. Indole inhibitors of human nonpancreatic secretory phospholipase A₂. 3. Indole-3-glyoxamides. *J. Med. Chem.* **1996**, *39*, 5159–75.
- (12) Hagishita, S.; Yamada, M.; Shirahase, K.; Okada, T.; Murakami, Y.; Ito, Y.; Matsuura, T.; Wada, M.; Kato, T.; et al. Potent inhibitors of secretory phospholipase A₂: Synthesis and inhibitory activities of indolizine and indene derivatives. *J. Med. Chem.* **1996**, *39*, 3636–3658.
- (13) Schevitz, R. W.; Bach, N. J.; Carlson, D. G.; Chirgadze, S. E.; Hartley, L. W.; Jones, N. D.; Mihelich, E. D.; et al. Structure-based design of the first potent and selective inhibitor of human non-pancreatic secretory phospholipase A₂. *Nat. Struct. Biol.* **1995**, *2*, 458–65.
- (14) Scott, D. L.; White, S. P.; Browning, J. L.; Rosa, J. J.; Gelb, M. H.; Sigler, P. B. Structures of free and inhibited human secretory phospholipase A₂ from inflammatory exudate. *Science* **1991**, *254*, 1007–1010.
- (15) Singer, A. G.; Ghomashchi, F.; Le Calvez, C.; Bollinger, J.; Bezzine, S.; Rouault, M.; Sadilek, M.; Nguyen, E.; Lazdunski, M.; Lambeau, G.; Gelb, M. H. Interfacial kinetic and binding properties of complete set of human and mouse groups I, II, V, X, and XII secreted phospholipases A₂. *J. Biol. Chem.* **2002**, *277*, 48535–48549.
- (16) Smart, B. P.; Pan, Y. H.; Weeks, A. K.; Bollinger, J. G.; Bahnson, B. J.; Gelb, M. H. Inhibition of the complete set of mammalian secreted phospholipases A₂ by indole analogs: A structure-guided study. *Bioorg. Med. Chem.* **2004**, *12*, 1737–1749.
- (17) Smart, B. P.; Oslund, R. C.; Walsh, L. A.; Gelb, M. H. The first potent inhibitor of mammalian group X secreted phospholipase A₂: Elucidation of sites for enhanced binding. *J. Med. Chem.* **2006**, *49*, 2858–60.
- (18) Pan, Y. H.; Yu, B. Z.; Singer, A. G.; Ghomashchi, F.; Lambeau, G.; Gelb, M. H.; Jain, M. K.; Bahnson, B. J. Crystal structure of human group X secreted phospholipase A₂. Electrostatically neutral interfacial surface targets zwitterionic membranes. *J. Biol. Chem.* **2002**, *277*, 29086–93.
- (19) Sawyer, J. S.; Beight, D. W.; Smith, E. C.; Snyder, D. W.; Chastain, M. K.; Tielking, R. L.; Hartley, L. W.; Carlson, D. G. Carbocyclic[indole] inhibitors of human nonpancreatic s-PLA₂. *J. Med. Chem.* **2005**, *48*, 893–896.
- (20) McMartin, C.; Bohacek, R. S. QXP: Powerful, rapid computer algorithms for structure-based drug design. *J. Comput.-Aided Mol. Des.* **1997**, *11*, 333–344.
- (21) Ogawa, T.; Seno, K.; Hanasaki, K.; Ikeda, M.; Ono, T. Compounds exhibiting X-type sPLA₂ inhibiting effect. U.S. Patent 7026318B2, 2006.
- (22) Jain, M. K.; Yuan, W.; Gelb, M. H. Competitive inhibition of phospholipase A₂ in vesicles. *Biochemistry* **1989**, *28*, 4135–4139.
- (23) Jain, M. K.; Yu, B.-Z.; Gelb, M. H.; Berg, O. G. Assay of phospholipase A₂ and their inhibitors by kinetic analysis in the scooting mode. *Med. Inflamm.* **1992**, *1*, 85–100.
- (24) Kitadokoro, K.; Hagishita, S.; Sato, T.; Ohtani, M.; Miki, K. Crystal structure of human secretory phospholipase A₂-IIA complex with the potent indolizine inhibitor 120-1032. *J. Biochem* **1998**, *123*, 619–623.
- (25) Ancian, P.; Lambeau, G.; Lazdunski, M. Multifunctional activity of the extracellular domain of the M-type (180 kDa) membrane receptor for secretory phospholipases A₂. *Biochemistry* **1995**, *34*, 13146–13151.

JM800422V